

# Silicate Layer Exfoliation in Polyolefin/Clay Nanocomposites Based on Maleic Anhydride Modified Polyolefins and Organophilic Clay

Naoki Hasegawa, Arimitsu Usuki

Toyota Central Research and Development Laboratories, Inc., 41-1, Nagakute, Aich, 480-1192, Japan

Received 25 September 2003; accepted 13 February 2004

DOI 10.1002/app.20459

Published online in Wiley InterScience (www.interscience.wiley.com).

**ABSTRACT:** Silicate layer exfoliation processes in maleic anhydride (MA) modified polyolefins were studied by using X-ray diffraction measurements, scanning electron microscopy, and transmission electron microscopy observations. Modified polyolefins grafted with 0.09–4.5 wt % MA groups intercalate into the organophilic clay galleries modified with stearyl ammonium ions. Molten MA-modified polypropylene continuously intercalates into the galleries and the

silicate layers exfoliate spontaneously without shear. However, the silicate layers maintain arranging parallel together, although the interlayer spacing expands over 10 nm. By adding shear, the silicate layers homogeneously disperse into MA-modified polypropylene matrix. © 2004 Wiley Periodicals, Inc. *J Appl Polym Sci* 93: 464–470, 2004

**Key words:** nanocomposites; clay; polyolefins

## INTRODUCTION

In recent years, organic–inorganic nanocomposites have attracted great interest to researchers because they frequently exhibit unexpected hybrid properties synergistically derived from the two components.<sup>1–14</sup> One of the most promising composite systems would be nanocomposites based on organic polymers and inorganic clay minerals consisting of silicate layers.<sup>4–14</sup> In our previous work, we synthesized nylon 6/clay nanocomposites (NCH), wherein 1-nm-thick silicate layers of clay minerals disperse homogeneously.<sup>4</sup> NCH exhibits various superior properties such as high strength, high modulus, and high heat resistance compared to nylon 6.<sup>4</sup> Since then, other polymer–clay nanocomposites such as polyimide,<sup>6</sup> epoxy resin,<sup>7</sup> polystyrene,<sup>8</sup> polycaprolactone,<sup>9</sup> acrylic polymer,<sup>10</sup> and polypropylene<sup>11</sup> were reported.

We reported silicate-layer exfoliation in polyolefins, such as polypropylene (PP) and polyethylene, is achieved by the introduction of small amounts of polar groups to nonpolar polyolefins.<sup>11a–d,12</sup> Exfoliated-type polyolefin/clay nanocomposites were able to be easily prepared by melt-compounding maleic anhydride (MA) modified polyolefins with organophilic clay ion-exchanged with alkylammonium ions. Since then, many kinds of polyolefin/clay nanocomposites

using modified polyolefins were prepared and their properties, especially mechanical and thermal properties, were examined. However, the exfoliation process of silicate layers in modified polyolefins was scarcely studied.<sup>13</sup> For polymer intercalation into the galleries of organophilic layered silicates, Giannelis et al. reported that polystyrene intercalates into the layered silicate galleries above its glass transition temperature with and without shear.<sup>8b</sup> In this case, polystyrene intercalates until the interlayer spacing of the layered silicates expands by approximately 1 nm but layered silicates do not exfoliate in the polystyrene matrix.

In this article, we study the dispersion process of silicate layers in polyolefin/clay nanocomposites based on MA-modified polyolefins and focus on spontaneous exfoliation of silicate layers.

## EXPERIMENTAL

### Materials

Purified Na-montmorillonite (Kunipia-F) was purchased from Kunimine Ind., Co. (Tokyo, Japan). Its cation exchange capacity is 119 meq./100 g. Stearylamine was purchased from Wako Pure Chemical Co. (Tokyo, Japan). MA-modified polyolefins used in this study are listed at Table I. The amounts of MA groups in the polyolefins were determined by titration by using KOH solution. The equivalent weights (molecular weight of polyolefin per one MA group) are calculated as follows: equivalent weight = (molecular weight of MA/wt % of MA group) × 100.

Correspondence to: N. Hasegawa (e0974@mosk.tytlabs.co.jp).

TABLE I  
Maleic Anhydride Modified Polyolefins

Main chain	Amount of maleic anhydride (wt%)	Equivalent weight (g/mol)	Weight-average molecular weight ( $M_w$ )	Melting point (°C)	Melt viscosity (cp @ 160°C)	Manufacturer	
U1010	PP	4.54	2,100	30,000	145	7,000	Sanyo Chemical
U1001	PP	2.26	4,300	40,000	154	16,000	Sanyo Chemical
U110TS	PP	0.61	16,000	12,000	145	100	Sanyo Chemical
U100TS	PP	0.31	32,000	10,000	145	120	Sanyo Chemical
PO1015	PP	0.20	49,000	209,000	—	—	Exxon Chemical
MP0620	EPR	0.55	18,000	269,000	—	—	Mitsui Chemical
MP0610	EPR	0.38	26,000	379,000	—	—	Mitsui Chemical
VA1820	EPR	0.09	110,000	336,000	—	—	Exxon Chemical
MA2	PP	0	—	—	164	—*	Mitubishi Chemical

MFR = 16g/10 min (JIS K6758).

### Organophilic clay

Organophilic montmorillonite ion-exchanged with stearyl ammonium ions was prepared by a typical method.<sup>11a</sup> It is termed C18-Mt. The interlayer spacing of C18-Mt was 2.20 nm measured by X-ray diffraction (XRD) measurement. The inorganic content was 69–71 wt % by measuring the weights before and after burning its organic component.

### Preparation of samples by melt-compounding

Polyolefin/clay nanocomposites were prepared by melt-compounding MA-modified polyolefin pellets or powder with C18-Mt powder by using twin-screw extruders. The inorganic contents of the samples were obtained by measuring the weights before and after burning their organic component. The compounding conditions and the inorganic contents are summarized in Table II.

### Preparation of samples without shear

Samples using U1001 and C18-Mt were prepared without adding shear as follows: Metal plates coated

with Teflon and spacers of 2 mm thickness were pre-heated at 200°C by using a hot press. A mixture of MA-modified PP U1001 powder and C18-Mt powder was set in the space between the metal plates and was heated for 2, 5, 10, and 60 min, respectively. After heating, the metal plates were put into water to cool the samples quickly, producing the sheet samples without shear. Their inorganic contents were approximately 5 wt %.

### Instruments

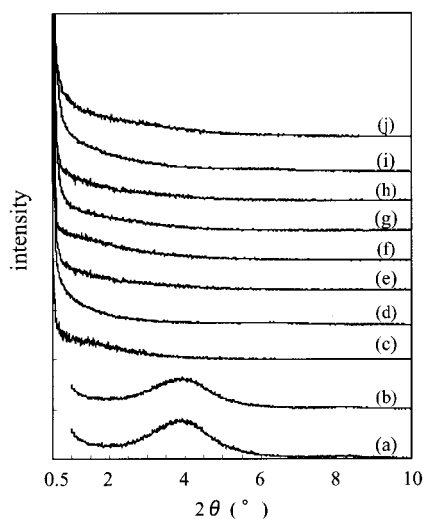
XRD measurements were performed by using a Rigaku RAD-B diffractometer with Cu-K $\alpha$  radiation generated at 30 kV and 30 mA. Transmission electron microscopy (TEM) observations were taken with a TEM 2000EX from JEOL. Scanning electron microscopy (SEM) observations were taken with a SEM JSM-890 from JEOL. Optical microscopy observations were taken by a BHS-751-P from Olympus Optical Co. Viscosity measurements were performed by using a dynamic spectrometer RDS II from Rheometrics Inc. The cone-plate diameter is 50 mm.

TABLE II  
Compounding Conditions

	Temperature (°C)	Screw rotation speed (rpm)	Extruder	Inorganic content (wt %)
U1010	150	240	S1KRC <sup>a</sup>	5.0
U1001	160	240	S1KRC	5.0
U110TS	150	240	S1KRC	4.8
U100TS	150	240	S1KRC	4.7
PO1015	190	240	S1KRC	2.1
MP0620	200	200	TEX30- $\alpha$ 45.5BW <sup>b</sup>	5.1
MP0610	200	200	TEX30- $\alpha$ 45.5BW	6.1
VA1820	150	240	S1KRC	2.8
MA2	200	240	S1KRC	4.4

<sup>a</sup> Screw length: 255 mm; L/D: 10.2; manufacturer: Kurimoto, Ltd.

<sup>b</sup> Screw length: 1365 mm. L/D:45.5; manufacturer: Japan Steel Works, Ltd.



**Figure 1** XRD patterns of (a) C18-Mt, (b) polypropylene/C18-Mt composite, (c) MA-modified polyolefin/C18-Mt nanocomposites using U1010, (d) U1001, (e) U110TS, (f) U100TS, (g) PO10105, (h) MP0620, (i) MP0610, (j) VA1820.

## RESULTS AND DISCUSSION

### Influence of amounts of maleic anhydride groups and molecular weight

Figure 1 shows XRD patterns of C18-Mt, PP/C18-Mt composite, and MA-modified polyolefin/C18-Mt nanocomposites in the range of  $2\theta = 0.5\text{--}10^\circ$ . In the PP/C18-Mt composite [Fig. 1(b)], an apparent peak is observed at  $2\theta = 4^\circ$  ( $d = 2.2$  nm), corresponding to the (001) plane reflection of stacked silicate layers. The interlayer spacing is not different from that of C18-Mt [Fig. 1(a)], indicating that PP does not intercalate into the C18-Mt galleries. On the other hand, in the MA-modified polyolefin/clay nanocomposites, there is no apparent peak [Fig. 1(c–j)], indicating that polyolefins grafted with MA groups of 0.09–4.5 wt % intercalate into the C18-Mt galleries and the silicate layers exfoliate.

The driving force of MA-modified polyolefin intercalation into organophilic clay galleries is thought to be hydrophilic interaction between MA groups and the polar silicate layer surfaces. In the case of VA1820 grafted with the smallest amount of MA of 0.09 wt %, the equivalent weight is 110,000. Thus, one MA group promotes diffusion of polyolefins with a molecular weight of more than 100,000 into organophilic clay galleries.

Figure 2 shows the TEM images of modified polyolefin/clay nanocomposites, wherein the black lines represent cross sections of silicate layers with 1 nm thickness, whereas the gray region represents polyolefin matrix. In the TEM images of the nanocomposites using U1001, U1010, PO1015, MP0620, MP0610, and VA1820, the silicate layers are found to exfoliate and

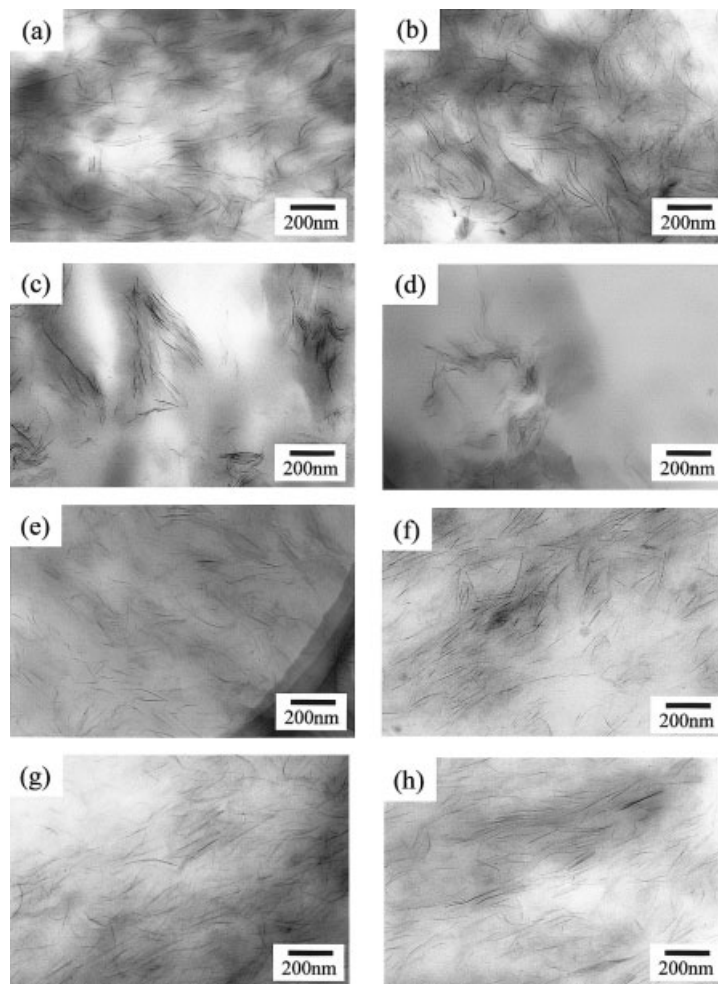
disperse homogeneously at the nanometer level. On the other hand, aggregates of multisilicate layers are observed in the TEM images of the nanocomposites by using U110TS and U100TS [Fig. 2(c, d)], although the silicate layers exfoliate as the XRD measurement results indicate. It is thought that, in the cases of U110TS and U100TS, the shear force during melt-compounding is not enough to disperse silicate layers into the matrix homogeneously, because the molecular weight of U110TS and U100TS are lower and their melt viscosities are much lower compared to the other polyolefins.

### Dispersion behaviors of silicate layers without shear

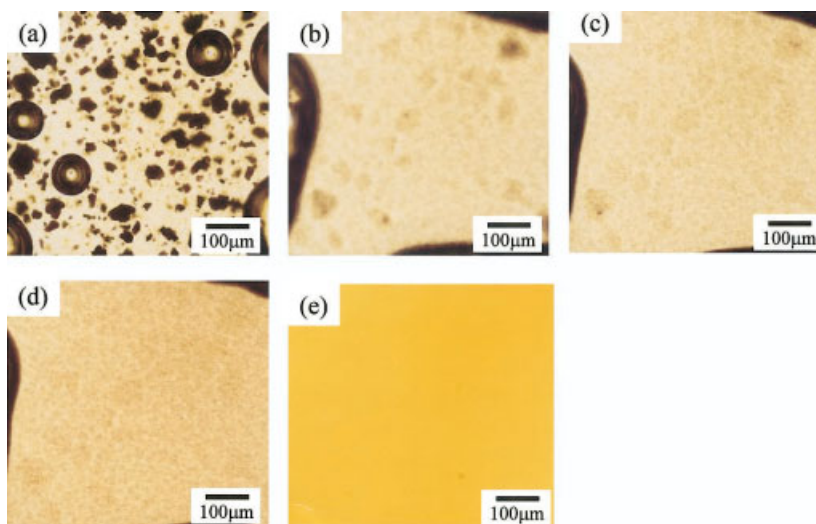
The TEM images in Figure 2 suggest that silicate layer dispersion process in MA-modified polyolefins during melt-compounding might consist of three steps, that is, (1) MA-modified polyolefin intercalation to organophilic clay galleries, (2) exfoliation of silicate layers, and (3) homogeneous dispersion of the silicate layers into the matrix by shear. To study these three dispersion steps separately, first we examined the silicate layer dispersion under no-shear in U1001/C18-Mt samples.

Figure 3 shows the optical micrographs of C18-Mt powder in molten U1001. Mixture of U1001 powder and C18-Mt powder, whose inorganic content was 10 wt %, was sandwiched between two cover glasses and was set in a hot stage mounted on an optical microscope at 200°C. U1001 completely melted in initial 20 s. In the optical micrograph after 30 s [Fig. 3(a)], the shapes of C18-Mt powder are relatively apparent. As the time passes, the shapes of C18-Mt powder become unapparent. It is thought that molten U1001 penetrates into the space between layered silicate particles composing C18-Mt powder. In the micrograph after 60 min [Fig. 3(d)], C18-Mt powder seems to disperse uniformly at the micrometer level, but which is much less homogeneous compared to the sample prepared by melt-compounding [Fig. 3(e)].

Figure 4 shows the SEM images of the sample prepared without shear at 200°C for 60 min. Frozen sections of the sample were prepared by using liquid nitrogen and then the polymer resin on the frozen section surface was removed by plasma etching by using oxygen gas to observe inorganic silicate layers clearly. There are white regions of 10–50  $\mu\text{m}$  in Figure 4(a), which are aggregates of silicate layers jutting out from the polymer matrix [Fig. 4(c)]. It is shown that the silicate layers do not disperse homogeneously in the matrix; that is, the silicate layer aggregates of C18-Mt powder maintained after molten U1001 penetrate into C18-Mt powder without shear. The silicate layer particles composing the aggregates, shown in



**Figure 2** TEM images of MA-modified polyolefin/C18-Mt nanocomposites. (a) U1010, (b) U1001, (c) U110TS, (d) U100TS, (e) PO10105, (f) MP0620, (g) MP0610, (h) VA1820.



**Figure 3** Optical micrographs of C18-Mt powder in molten U1001 at 200°C (a) after 30 s, (b) after 2 min, (c) after 5 min, (d) after 60 min. (e) Molten U1001/C18-Mt sample prepared by melt-compounding.

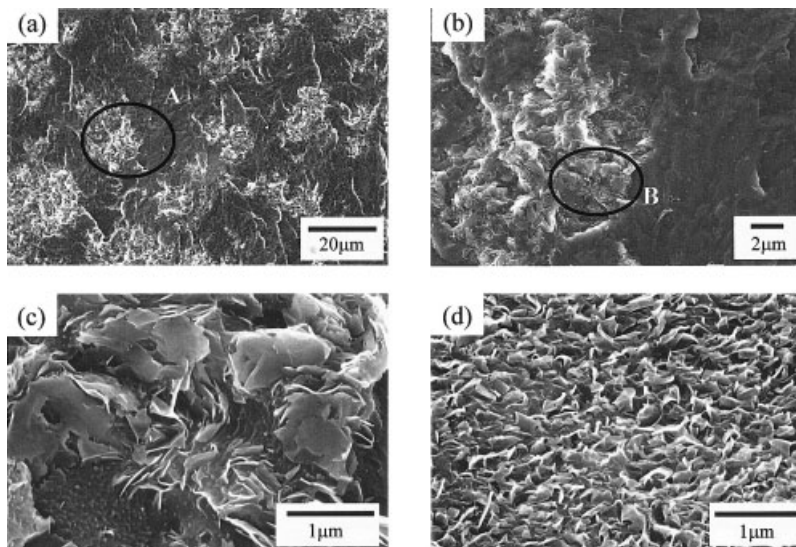


**Figure 4** (a) SEM images of the sample prepared from U1001 powder and C18-Mt powder without shear. (b) Magnified figure of region A. (c) Magnified figure of region B. (d) PO1015/C18-Mt sample prepared by melt-compounding.

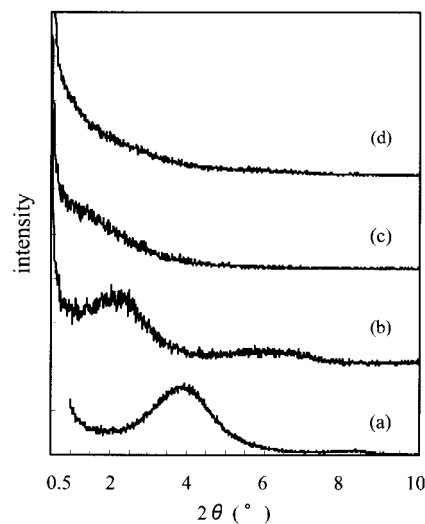
Figure 4(c), might consist of multisilicate layers stacking during the plasma etching, which are much larger than those in PO1015/C18-Mt sample prepared by melt-compounding, as shown in Figure 4(d).

Figure 5 shows the XRD patterns of U1001/C18-Mt samples prepared without shear at 200°C in the range of  $2\theta = 0.5\text{--}10^\circ$ . In the sample prepared for 2 min, a broad peak is observed around  $2\theta = 2^\circ$  and the peak corresponding to C18-Mt is not observed. It is shown that molten U1001 intercalated into the whole C18-Mt galleries for 2 min and that layered silicates intercalated with U1001 formed, whose interlayer spacing expands by  $\approx 1$  nm from that of C18-Mt. Molten U1001 might quickly intercalate into the C18-Mt galleries just after it penetrates into C18-Mt powder, because the molecular weight of U1001 is not high and the mobility in the molten state may be high. On the other hand, in the sample prepared for 5 and 60 min, no apparent peak is observed. Figure 6(a) shows the TEM images of the sample prepared for 60 min. The silicate layers are found to exfoliate and the spacing between silicate layers expanded over 10 nm. However, the silicate layers do not disperse uniformly into the U1001 matrix, wherein several silicate layers maintain arranging parallel together. The parallel structures of the silicate layers are thought to come from layered structures of C18-Mt.

The above-mentioned results indicate that, even under nonshear, molten modified PP penetrates into the space between layered silicates in organophilic clay powder and continuously intercalates into layered silicate galleries and silicate layers spontaneously exfoliate.

To confirm the universality of spontaneous exfoliation of silicate layers as shown in MA-modified PP, we

investigated whether spontaneous exfoliation also occurs in nylon 6. Nylon 6, as is known, forms exfoliated-type clay nanocomposites by melt-compounding with organophilic clay, such as C18-Mt.<sup>14</sup> The sample using nylon 6 powder and C18-Mt powder were prepared without shear at 240°C for 60 min by the same method preparing U1001/C18-Mt samples. Figure 6(b) is the TEM image of the nylon 6/C18-Mt sample. The TEM image gives that the silicate layers of C18-Mt also exfoliate in nylon 6 as well as in MA-modified PP. It is indicated that silicate layers spontaneously exfoliate without shear in the polymers, which form exfoliated-type clay nanocomposites by melt-compounding.



**Figure 5** XRD patterns of (a) C18-Mt, (b) the samples prepared from U1001 powder and C18-Mt powder without shear at 200°C for 2 min, (c) for 5 min, (d) for 60 min.

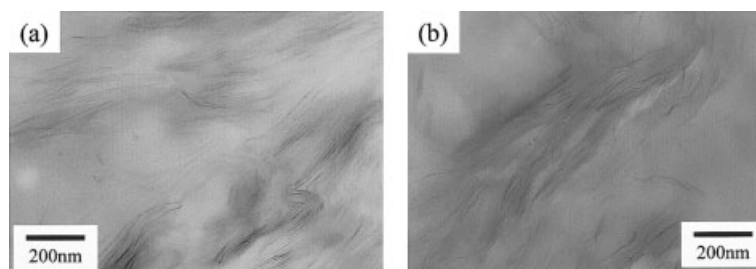


**Figure 6** TEM images of the samples prepared without shear (a) from U1001 powder and C18-Mt powder, (b) from nylon 6 powder and C18-Mt powder.

### Dispersion behaviors of silicate layers with shear

To investigate the influence of shear on silicate layer dispersion, silicate layer dispersion was examined before and after adding shear. The sheet samples using U1001 and C18-Mt prepared without shear at 200°C for 60 min were set between a cone-plate in a rotational viscometer at 180°C under nitrogen. Steady shear was added to the samples at constant shear rates of 20, 50, and 100  $\text{s}^{-1}$ , respectively. Figure 7 shows the changes with time of viscosity during the addition of shear to the samples. In the case of a shear rate of 20  $\text{s}^{-1}$ , the viscosity is slowly decreasing. After about 8 min, a small amount of the sample began to stick out from the cone-plate and the measurement was ceased after 10 min. In the cases of shear rates of 50 and 100  $\text{s}^{-1}$ , the viscosities rapidly decrease initially  $\approx 2$  min and then the viscosities become constant. In these two cases, parts of the samples also stick out from the cone-plate after about 6 and 7 min, respectively, and the measurements were ceased. Figure 8 shows the TEM images of the samples after adding shear. The samples were taken out from the cone-plate before U1001 solidification to avoid the cone-plate adhesion, so the TEM images do not strictly show the silicate layer dispersion just after completing the measurements. In the sample prepared at a shear rate of 20  $\text{s}^{-1}$ , a lot of silicate layers are found to arrange parallel, as shown in Figure 8(a), although small parts of silicate layers disperse disorderly. The arranging structures of silicate layers still remained as with the sample before adding shear as shown in Figure 6(a). During the addition of shear at a shear rate of 20  $\text{s}^{-1}$ , it is guessed that the arranging structure of silicate layers may be changing to disorder, because the viscosity is continuously decreasing. However, silicate layers do not homogeneously disperse in 10 min. On the other hand, in the samples prepared at shear rates of 50 and 100  $\text{s}^{-1}$ , most of silicate layers are found to disperse homogeneously, as shown in Figure 8(b, c), although small parts of silicate layers are maintained by arranging parallel together. It is thought that the initial rapid drops in the viscosities are presumably due to col-

lapses of arranging structure of silicate layers and subsequent silicate layer orientation to the shear flow, and that the silicate layers homogeneously disperse in the initial 2 min because the viscosity is almost constant after 2 min. These results indicate that the exfoliated silicate layers that arrange parallel disperse into the matrix homogeneously by adding shear at a low shear rate of 50  $\text{s}^{-1}$  for a short time of 2 min.

### CONCLUSION

Modified polyolefins grafted with 0.09–4.5 wt % MA groups intercalate into the galleries of C18-Mt organomodified with stearyl ammonium ions. Even under nonshear, molten modified PP U1001 continuously intercalates into the galleries of C18-Mt and then the silicate layers of C18-Mt exfoliate spontaneously. The

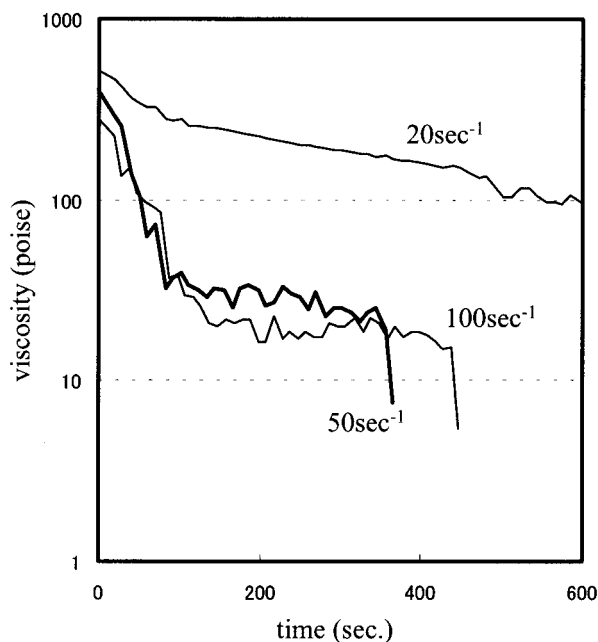


**Figure 7** The changes with time of viscosity during adding shear to the samples prepared from U1001 powder and C18-Mt powder without shear.

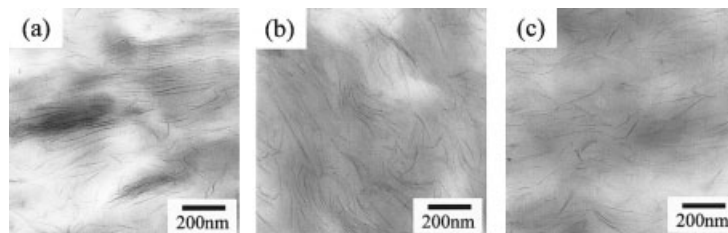


**Figure 8** TEM images of the samples after adding shear at shear rates of (a)  $20 \text{ s}^{-1}$ , (b)  $50 \text{ s}^{-1}$ , (c)  $100 \text{ s}^{-1}$ .

silicate layers maintain arranging parallel together without shear, although the spacing between the silicate layers expand over 10 nm. In the case of U1001, silicate layers disperse into the matrix homogeneously by adding shear at a shear rate of  $50 \text{ s}^{-1}$  for 2 min.

## References

- Schmidt, H. in *Polymer Based Molecular Composites*; Schaefer D. W.; Mark, J. E., Eds; Material Res. Society: Pittsburgh, PA, 1990; p.3.
- Schmidt, H. K. *Macromol Sympos.* 1996, 101, 333–342.
- Beecroft, L. L.; Ober, C. K. *Chem Mater* 1997, 9, 1302.
- (a) Okada, A.; Usuki, A. *Mater. Sci. Eng.*, 1995, C3, 109; (b) Usuki, A.; Kawasumi, M.; Kojima, Y.; Fukushima, Y.; Okada, A.; Kurauchi, T.; Kamigaito, O. *J Mater Res* 1993, 8, 1179; (c) Kojima, Y.; Usuki, A.; Kawasumi, M.; Fukushima, Y.; Okada, A.; Kurauchi, T.; Kamigaito, O. *J Mater Res* 1993, 8, 1185.
- (a) Giannelis, E. P. *Adv Mater.* 1996, 8, 29; (b) Lagaly, G., *Appl Clay Sci* 1999, 15, 1. (b) LeBaron, P. C.; Wang, Z.; Pinnavaia, T. J. *Appl Clay Sci* 1999, 15, 11.
- Yano, K.; Usuki, A.; Okada, A.; Kurauchi, T.; Kamigaito, O. *J Polym Sci, Part A: Polym Chem* 1993, 31, 2493.
- (a) Usuki, A.; Mizutani, T.; Fukushima, Y.; Fujimoto, M.; Fukumori, K.; Kojima, Y.; Sato, N.; Kurauchi, T.; Kamigaito, O. *U.S. Pat* 4,889,885, 1989; (b) Wang, M. S.; Pinnavaia, T. J. *Chem Mater* 1994, 6, 468; (c) Lan, T.; Pinnavaia, T. J. *Chem Mater* 1994, 6, 2216; (d) Lan, T.; Kaviratona, P. J.; Pinnavaia, T. J. *Chem Mater* 1995, 7, 2214; (d) Kelly, P.; Akelah, A.; Qutubuddin, S.; Moet, A. *J Mater Sci* 1994, 29, 2274.
- (a) Vaia, R. A.; Isii, H.; Giannelis, E. P. *Chem Mater.* 1993, 5, 1694; (b) Vaia, R. V.; Jandt, K. D.; Edward, J. K. Giannelis, E. P. *Macromolecules* 1995, 28, 8080; (c) Moet, A.; Akelah, A. *Mater. Lett.* 1993, 18, 97; (d) Weiner, M. W.; Chen, Hua; Giannelis, E. P.; Sogah, D. Y. *J Am Chem Soc* 1999, 122, 1615; (e) Hasegawa, N.; Okamoto, H.; Kawasumi, M.; Usuki, A. *J Appl Polym Sci* 1999, 74, 3359.
- Messersmith, P. B.; Giannelis, E. P. *J Polym Sci, Part A; Polym Chem* 1995, 33, 1047.
- Biasci, L.; Aglietto, M.; Ruggeri, G.; Ciardelli, F. *Polymer* 1994, 35, 3296.
- (a) Kawasumi, M.; Hasegawa, N.; Kato, M.; Usuki, A.; Okada, A. *Macromolecules* 1997, 30, 6333; (b) Hasegawa, N.; Kawasumi, M.; Kato, M.; Usuki, A.; Okada, A. *J Appl Polym Sci* 1998, 67, 87; (c) Kato, M.; Usuki, A.; Okada, A. *J Appl Polym Sci* 1997, 66, 1781; (d) Hasegawa, N.; Okamoto, H.; Kato, M.; Usuki, A. *J Appl Polym Sci* 2000, 78, 1918; (e) Bergman, J. S.; Chen, H.; Giannelis, E. P.; Thomas, M. G.; Coates, G. W.; *Chem. Commun.* 1999, 21, 2179. (f) Heinemann, J.; Reichert, P.; Thomann, R.; Mülhaupt, R. *Macromol Rapid Commun* 1999, 20, 423.
- Hasegawa, N.; Okamoto, H.; Kawasumi, M.; Kato, M.; Tsukigase, A.; Usuki, A. *Macromol Mater Eng* 2000, 280/281, 76.
- Dennis, H. R.; Hunter, D. L.; Chang, D.; Kim, S.; White, J. L.; Cho, J. W.; Paul D.R. *Polymer* 2001, 42, 9513.
- Liu, L.; Qi, Z.; Zhu, X. *J Appl Polym Sci* 1999, 71, 1133.